Supplemental Table 1 : PCR primers used to build the different genetic constructs

Primer name	Primer sequence
UserPIP2;7Fw	5'–GGCTTAAXATGTCGAAAGAAGTGAGCGAA–3'
UserPIP2;7Rv	5'–GGTTTAAXTTAATTGGTTGCGTTGCTTCGGA–3
UserSYP61Fw	5'–GGCTTAAXATGTCTTCAGCTCAAGATCCAT–3'
UserSYP61Rv	5'–GGTTTAAXGGTCAAGAAGACAAGAACGAAT–3'
UserSYP61SP2Rv	5'–GGTTTAAXTTATCCAGCTTTCTTCATTACCAT–3'
UserSYP121Fw	5'–GGCTTAAXATGAACGATTTGTTTTCCAGCTC–3'
UserSYP121Rv	5'–GGTTTAAXTCAACGCAATAGACGCCTTGC–3'
DtopoSYP121SP2Rv	5'–ACATGTCCATTTTCGCGTGTTCTT–3'
DtopoSYP121SP2Fw	5'–CACCATGAACGATTTGTTTTCCAGCTC–3'
DtopoPIP2;7Fw	5'–CACCATGTCGAAAGAAGTGAGCGAA–3'
DtopoPIP2;7Rv	5'–TAATGTCGAAAGAAGTGAGCGAA–3'
attB3AtSYP121Fw	5'–GGGGACAACTTTGTATAATAAAGTTGTAATGAACGATTTGTTTTCCAGC–3'
attB2AtSYP121Rv	5'–GGGGACCACTTTGTACAAGAAAGCTGGGTTTCAACGCAATAGACGCCTTGC–3'
attB1AtPIP27Fw	5'–GGGGACAAGTTTGTACAAAAAAGCAGGCTTAATGTCGAAAGAAGTGAGCGAA–3'
attB4AtPIP27Rv	5'–GGGGACAACTTTGTATAGAAAAGTTGGGTGTTAATTGGTTGCGTTGCTTCG–3'
attB4AtSYP121Rv	5'–GGGGACAACTTTGTATAGAAAAGTTGGGTGTCAACGCAATAGACGCCTTGC–3'
attB1AtSYP121Fw	5'–GGGGACAAGTTTGTACAAAAAAGCAGGCTTAATGAACGATTTGTTTTCCAGC–3'
attB3AtSYP61Fw	5'–GGGGACAACTTTGTATAATAAAGTTGTAATGTCTTCAGCTCAAGATCCA–3'
attB2AtSYP61Rv	5'–GGGGACCACTTTGTACAAGAAAGCTGGGTTTTAGGTCAAGAAGACAAGAAC–3'
attB1AtPIP2;7ΔNtFw	5'–GGGGACAAGTTTGTACAAAAAAGCAGGCTTAATGTTCTACAGAGCTCTCATCGCT–3'
attB2AtPIP27ΔCtRv	5'–GGGGACCACTTTGTACAAGAAAGCTGGGTTTATGTATTGGTGGTAAGCTGC–3'
attB2AtPIP27W/sRv	5'–GGGGACCACTTTGTACAAGAAAGCTGGGTTATTGGTTGCGTTGCTTCG–3'
attB1AtSYP61Fw	5'–GGGGACAAGTTTGTACAAAAAAGCAGGCTTAATGTCTTCAGCTCAAGATCCA–3'
pDONRP4-PIP2;7pro-P1RFw	5'–GGGGACAACTTTGTATAGAAAAGTTGGATGAAATCTTATTGATTACTACTAG–3'
pDONRP4-PIP2;7pro-P1RRv	5'–GGGGACTGCTTTTTTGTACAAACTTGAGACGACGACAGTGTATCTCTTCTG–3'
pDONRP2R-PIP2;7-P3Fw	5'–GGGGACAGCTTTCTTGTACAAAGTGGGGATGTCGAAAGAAGTGAGCGAAGAAG–3'
pDONRP2R-PIP2;7-P3Rv	5'–GGGGACAACTTTGTATAATAAAGTTGGTTAATTGGTTGCGTTGCTTCGGAAC–3'

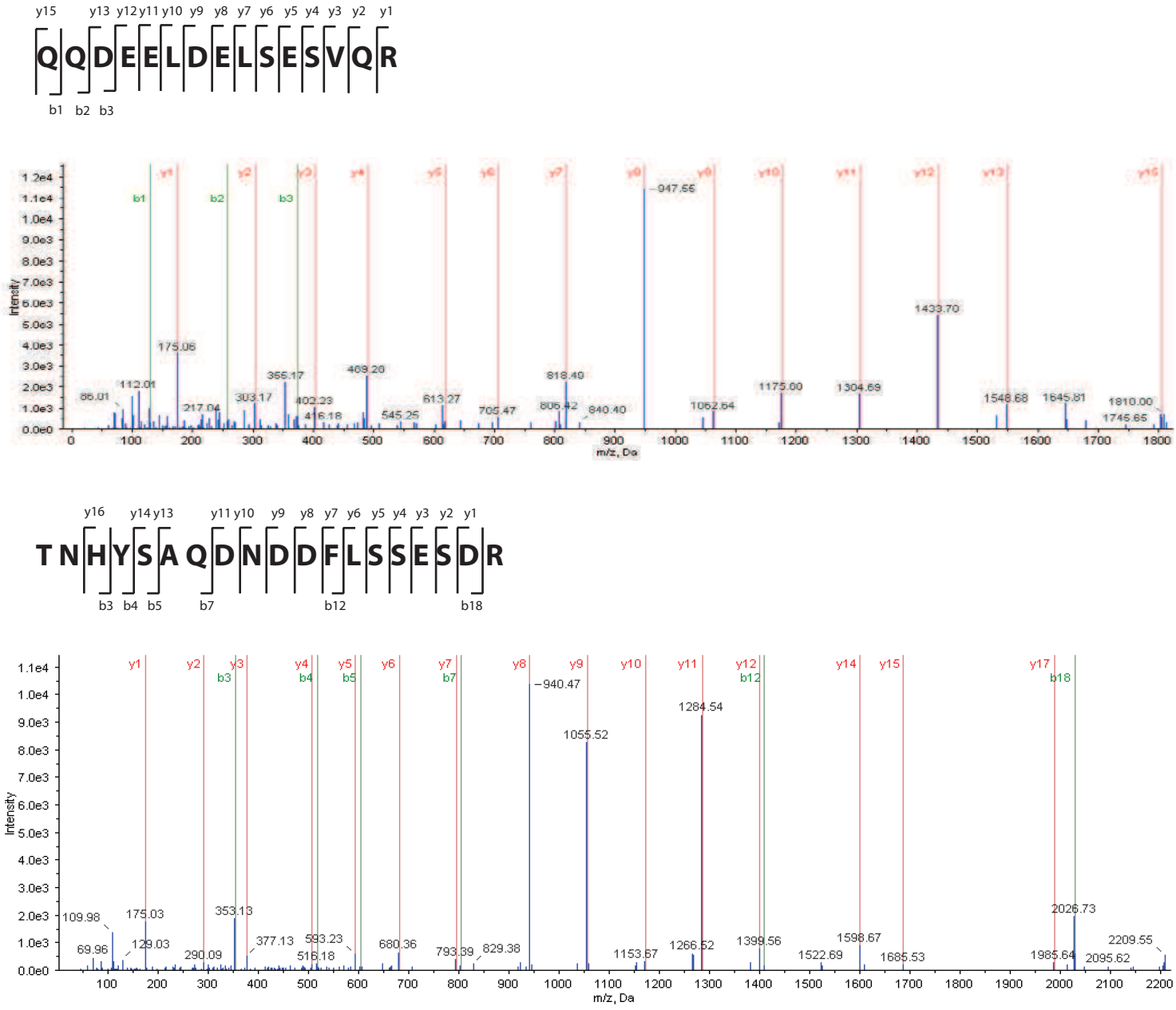

Supplemental Figure 1. Identification of ZmSYP61 as putative interactor of ZmPIP2;6 by affinity chromatography coupled to Maldi/TOF-TOF analysis.

The two peptides found in the elution fraction that could be unambiguously attributed to ZmSYP61 are shown. Given the quality of their MS-MS dissociation spectra, both peptides were identified with over 99% confidence.

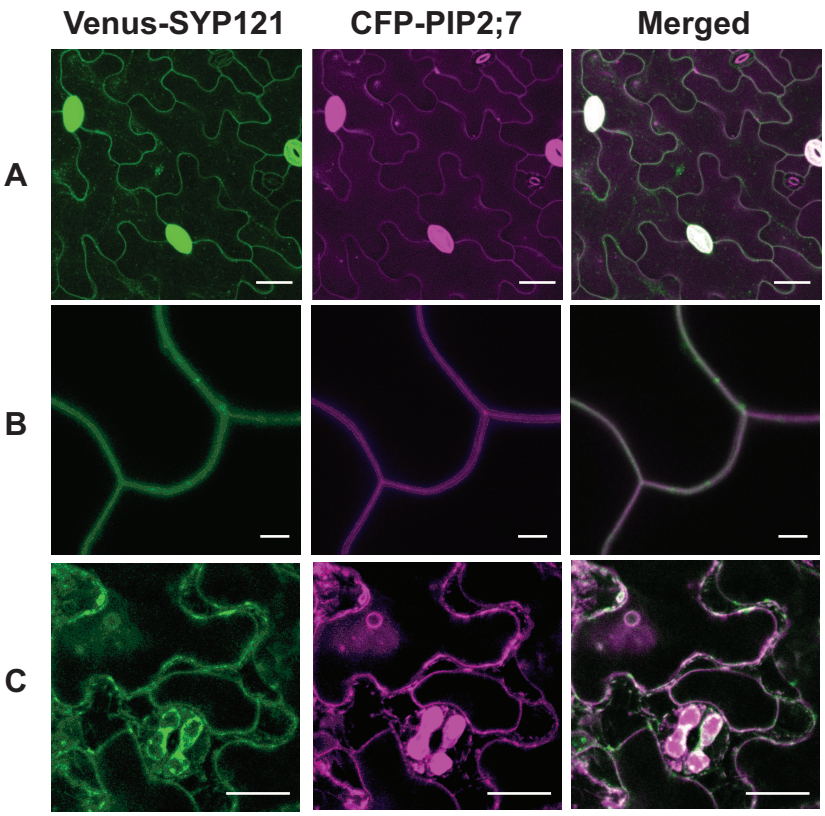

Supplemental Figure 2. Colocalization of SYP121 and PIP27.

(A-B) Colocalization of SYP121 and PIP2;7 expressed from *p35S:Venus-SYP121* and *p35S:CFP-PIP2;7* constructs in cotyledon epidermal cells. In control conditions, SYP121 and PIP2;7 colocalized in the plasma membrane. Images are maximum projections of three-dimensional reconstructions. **(C)** Venus-SYP121 and CFP-PIP2;7 reporters in cotyledon epidermal cells after 300 mM mannitol treatment for 3 min. This treatment triggered plasmolysis of the cells. Note that SYP121 still colocalizes with Venus-PIP2;7 in the plasmolyzed plasma membrane. Bars= 15 μm (A and C), 3 μm (B)

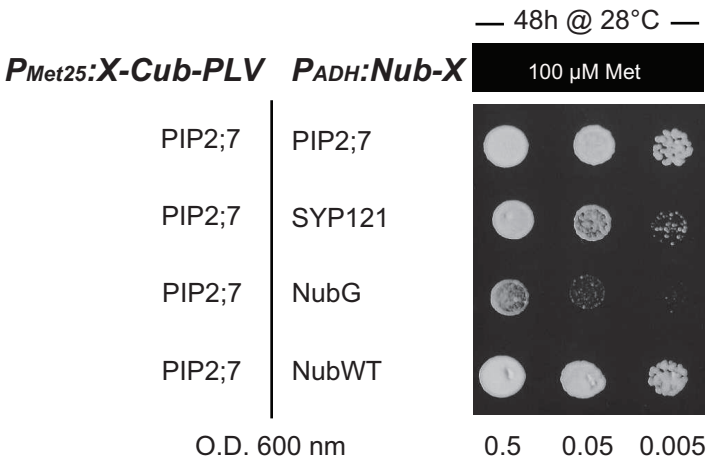

Supplemental Figure 3. Mating-based split-ubiquitin assays demonstrating PIP2;7 and SYP121 interaction.

Yeast coexpressing the PIP2;7-Cub-PLV/NubG-SYP121 grows similarly to the strain coexpressing the PIP2;7-Cub-PLV/NubG-PIP2;7 pair while no growth was observed for the negative control (see Methods for details). These experiments were repeated three times with independent biological replicates. Yeast growth on a single representative plate is shown.

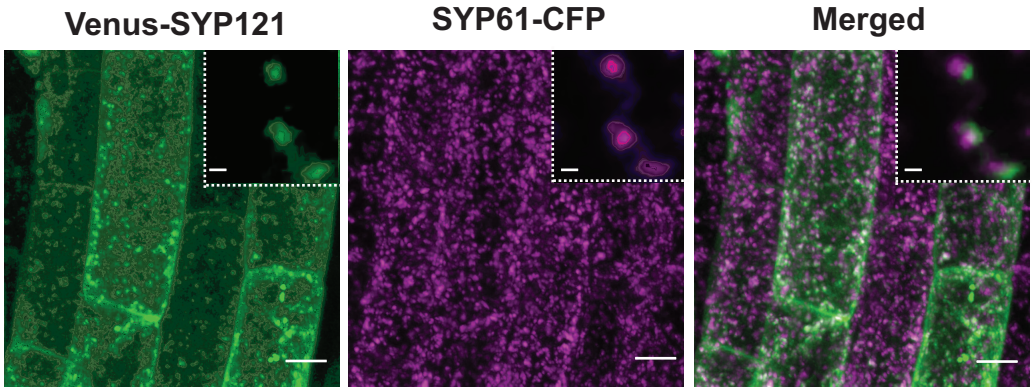

Supplemental Figure 4. Colocalization of SYP61 and SYP121 expressed from *pSYP61:SYP61-CFP* and *p35S:Venus-SYP121* constructs in elongated primary root cells.

SYP61 and SYP121 colocalized in the plasma membrane and in an endomembrane compartments (TGN). Merged images show a partial overlap of Venus-SYP121 and SYP61-CFP proteins at the TGN level and a weak colocalization in the plasma membrane. Images are maximum projections of three-dimensional reconstructions. Insets: close-up views of the fluorescently tagged TGN/EE structures. A partial overlap of SYP61-CFP and Venus-SYP121 within individual endosomes and colocalization in the middle of the endosomal structure are visible. Bars = 10 μm (main panels), 1 μm (insets).

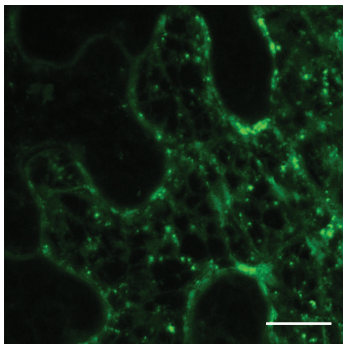

Supplemental Figure 5. Subcellular localization of transiently expressed GFP-AtPIP2;7ΔNΔCter in tobacco epidermal cells 48 h after leaf infiltration. Bar = 10 μm.

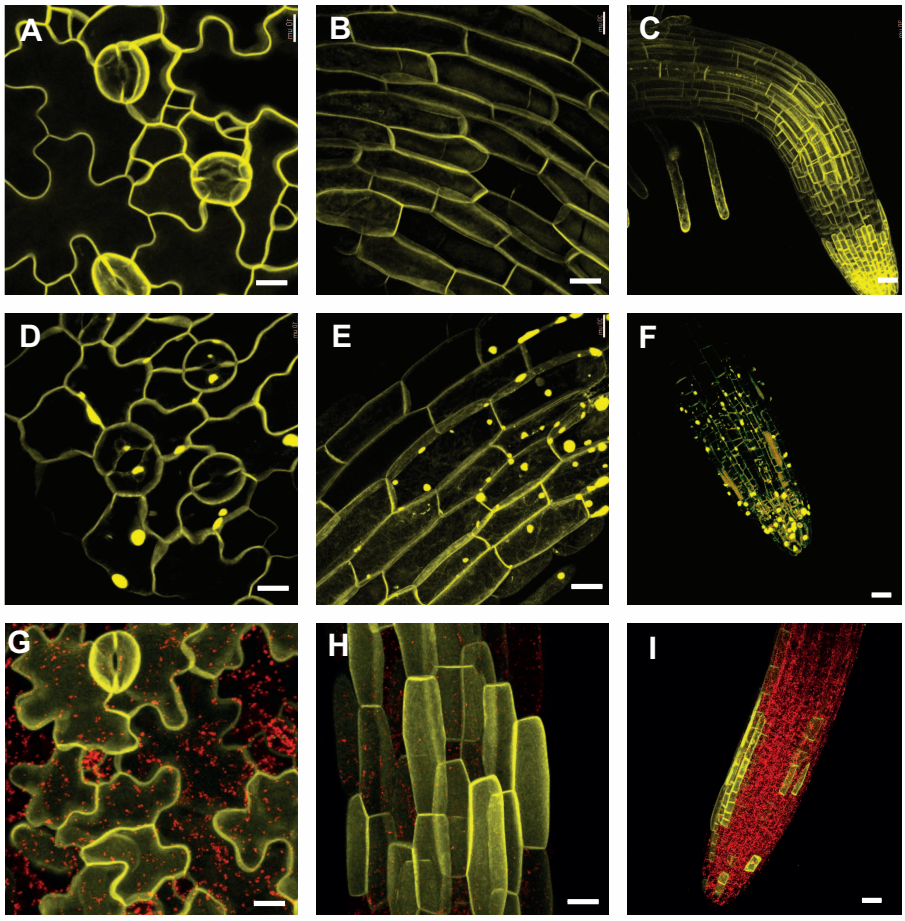

Supplemental Figure 6. Mistargeting of overexpressed Venus-AtPIP2;7 in *osm1* compared to WT backgrounds and phenotype complementation.

(A-C) Localization at the plasma membrane of Venus-PIP2;7 in a wild-type (C24) background in the epidermis (A), hypocotyl (B), and root tip (C) in 7-day-old seedlings.

(D-F) Localization in the plasma membrane and OSER structures of Venus-PIP2;7 in the *osm1* line in the epidermis (D), hypocotyl (E), and root tip (F) in 7-day-old seedlings.

(G-I) The *pSYP61:SYP61-CFP* construct rescues the OSER-inducing phenotype. Venus-PIP2;7-trapping in OSER structures is no longer observed in *osm1* upon coexpression of SYP61-CFP (in red) in the epidermis (G), hypocotyl (H), and root tip (I) of 7-day-old seedlings. Bars = 12 µm (A, B, D, E, G and H) and 15 µm (C, F and I).

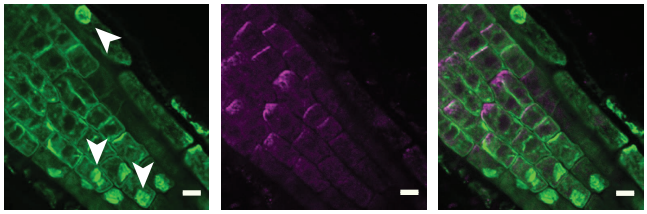

Supplemental Figure 7. Immunolocalization of Venus-PIP2;7 and PIN2 proteins in the *osm1* background.

Whole-mount in situ immunolocalization of Venus-PIP2;7 proteins in *osm1*. Venus-PIP2;7 accumulated in OSER structures (white arrowheads). Coimmunolocalization of PIN2 proteins in this background revealed that PIN2 still displayed a polar plasma membrane localization and did not occur in OSER structures. Bars = 5 μm.

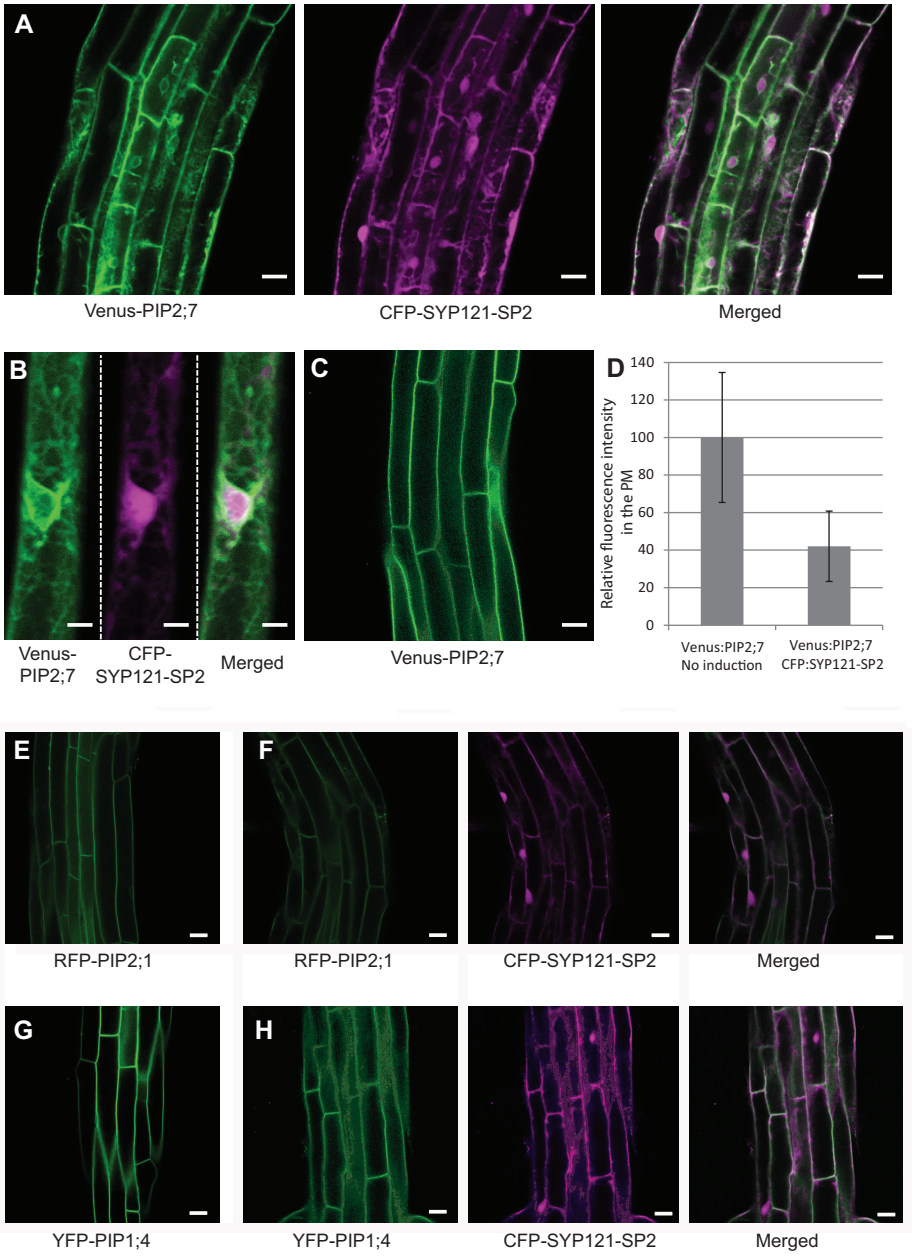

Supplemental Figure 8. Effect of the SYP121-Sp2 fragment on the subcellular localization of PIP fusion proteins.

(A) Venus-PIP2;7 in primary roots upon coexpression with a CFP-SYP121-Sp2-dominant negative fragment. Note the intracellular accumulation of Venus-PIP2;7 due to the coexpression with the SP2 fragment.

(B) Close-up showing ER retention of Venus-PIP2;7 upon coexpression with the CFP-SYP121-Sp2 fragment.

(C) Same as in A and B, but without induction of the CFP-SYP121-Sp2 expression (no β-estradiol treatment). In this case, Venus-PIP2;7 traffics properly to the plasma membrane and does not accumulate intracellularly.

(D) Relative Venus-PIP2;7 fluorescence intensity measurement in the plasma membrane (mean ± S.D.) without (n= 47 cells) or after induction of CFP-SYP121-Sp2 (n=70 cells). Coexpression of Venus-PIP2;7 and CFP-SYP121-Sp2 resulted in a 60% decrease in the Venus fluorescence at the plasma membrane.

(E) RFP-PIP2;1 labeling in the plasma membrane of the mature root zone.

(F) The subcellular localization and abundance of RFP-PIP2;1 is altered by coexpression of *RFP-PIP2;1* and *CFP-SYP121-Sp2* fragments.

(G) YFP-PIP1;4 labelling in the plasma membrane of the mature root zone.

(H) Alteration of the the subcellular localization and abundance of YFP-PIP1;4 proteins upon coexpression with *CFP-SYP121-Sp2* fragments.

Bars = 20 µm (A and C), 15 µm (E, F, G and H) and 5 µm (B).

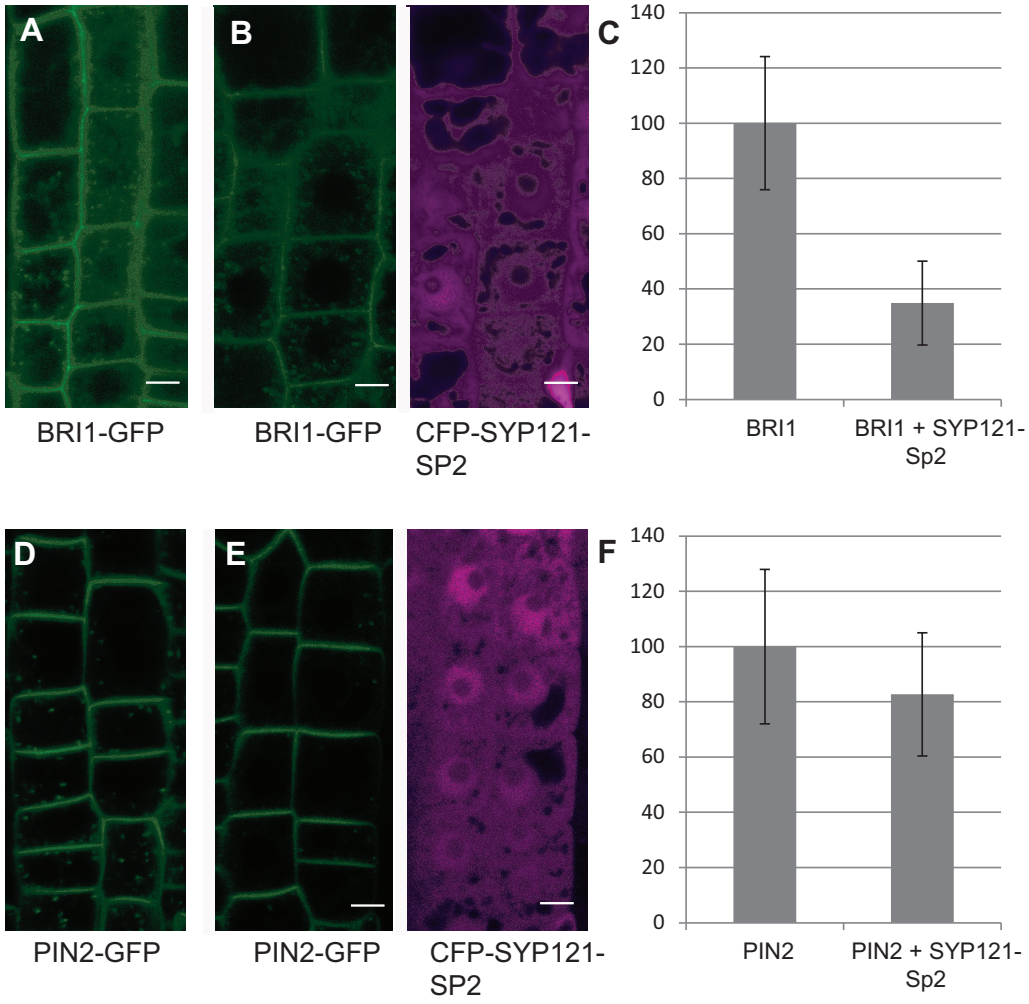

Supplemental Figure 9. Effect of SYP121-Sp2 fragments on PIN2 and BRI1 subcellular localization.

(A) BRI1-GFP localization under control conditions (no β-estradiol treatment). Both the plasma membrane and intracellular vesicles are labeled.

(B) Detection of BRI1-GFP upon coexpression with a CFP-SYP121-Sp2 dominant-negative fragment taken with the same confocal settings as in (A). The BRI1-GFP signal intensity is reduced.

(C) Relative BRI1-GFP fluorescence intensity measurement in the plasma membrane (mean ± S.D.) without (n=47) or after induction of CFP-SYP121-Sp2 (n=60). Coexpression of BRI1-GFP and CFP-SYP121-Sp2 resulted in a ~60% decrease in Venus fluorescence intensity in the plasma membrane.

(D) PIN2-GFP polar localization under control conditions (no β-estradiol treatment).

(E) PIN2-GFP upon coexpression with a CFP-SYP121-Sp2 dominant-negative fragment. Same confocal settings as in (D). Neither the polar localization, nor the signal intensity of PIN2-GFP were affected by the SYP121-Sp2 fragment.

(F) Relative PIN2-GFP fluorescence intensity measurement in the plasma membrane (mean ± S.D.) without (n=63 cells) or after induction of CFP-SYP121-Sp2 (n=83 cells). Coexpression with SYP121-Sp2 did not trigger a significant alteration in PIN2-GFP trafficking. Bars = 5 μm.

Supplemental Methods

Identification of proteins interacting with ZmPIP2;6

A Maize Black Mexican Sweet suspension cell line expressing 6His-cmyc-ZmPIP2;6 (Cavez et al., 2009) was used to identify interacting proteins. Microsomal proteins extracted from 14 day-old cells were solubilized using 1% octyl glucopyranoside and the 6His-cmyc-ZmPIP2;6 proteins were purified by Ni-affinity chromatography. A high number of contaminants were still present in the elution fraction after this affinity chromatography. Therefore, an immunoprecipitation with purified ZmPIP2;6 antibodies was performed that removed most of the contaminants. One hundred µl of purified anti-ZmPIP2;6 antibodies were added to the sample before overnight incubation at 4°C on a rotating wheel. Then 100 µl of Protein A Sepharose CL-4B resin (GE Healthcare Life Sciences, Piscataway, NJ) were added to a Micro Bio-Spin Chromatography column (Bio-Rad), washed with phosphate buffer saline (PBS) and incubated with the sample for 1 h at RT on a rotating wheel. After eight washes with 400 µl of solubilisation buffer and four washes with 400 µl of PBS, proteins were eluted in 1 ml elution buffer (15 mM glycine, 150 mM NaCl, pH 2,3 (HCl)). Precipitation with chloroform/methanol was then performed and the resulting pellet resuspended in 40 µl Triethylammonium bicarbonate 50 mM + 0.5 % (w/v) RapiGest (acid-cleavable surfactant used to enhance enzymatic digestion of proteins, Waters) by vortexing for 1 h. The sample was reduced with 25 mM Tris(2-carboxyethyl)phosphine for 1 h at 60°C, alkylated with 200 mM Methyl methanethiosulfonate (MMTS) for 15 min in the dark and digested with 1 µg trypsin O/N at 37°C. To pellet the RapiGest, the sample was incubated with 1 % Trifluoroacetic acid (TFA) for 45 min at 37°C and centrifuged at 130,000 g for 15 min at 4°C. Finally, the supernatant was dried in a speed-vac, resuspended in 0.1 % (w/v) TFA and analyzed by MALDI-TOF-TOF.

Proteins were identified with the MASCOT (Matrix Science, London, UK) searching algorithms using the monoisotopic peptide masses and a peptide mass tolerance of ± 200 ppm. Searching was performed on the *Zea mays* B73 database. Identified protein sequences having a confidence interval higher than 95 % were selected for a first BLAST analysis performed on the Uniref100 database (Uniprot) and a second BLAST analysis performed on the nr database (NCBI) using the Blast2GO software (Conesa et al., 2005).

Construction and transient expression of GFP-PIP2;7ΔNΔCter in tobacco epidermal cells.

The mutated version of PIP2;7 (PIP2;7ΔNΔCter, where amino acid residues 1-39 (cytosolic N terminus) and 263-280 (cytosolic C terminus) were deleted) was obtained by PCR amplification of the *PIP2;7* cDNA template with D-TOPO cloning-compatible primers. PCR fragments were recombined into a pENTR vector with the pENTR Directional TOPO Cloning Kit (Invitrogen) and further recombined into the pMDC43 destination vector (Curtis and Grossniklaus, 2003) by LR cloning (Invitrogen). The GFP-PIP2;7ΔNΔCter construct was introduced in *Agrobacterium tumefaciens* AGL1 strain and tobacco leaves were transfected by infiltration. Subcellular localization of GFP-PIP2;7ΔNΔCter proteins was visualized by confocal microscopy 48 h after leaf infiltration.

Whole-mount in situ protein localization

Whole-mount in situ immunolocalizations were carried out on 5-day-old seedlings with an automated procedure exactly as described (Sauer et al., 2006). This experiment was performed twice on independent samples originating from the same homozygous line.

References:

Cavez D, Hachez C, Chaumont F. (2009) Maize black Mexican sweet suspension cultured cells are a convenient tool for studying aquaporin activity and regulation. Plant Signal Behav. 4: 890-892

Conesa A, Götz S, García-Gómez JM, Terol J, Talón M, Robles M. (2005) Blast2GO: a universal tool for annotation, visualization and analysis in functional genomics research. Bioinformatics. **21:** 3674-3676.

Curtis, M.D., and Grossniklaus, U. (2003). A Gateway cloning vector set for high-throughput functional analysis of genes in planta. Plant Physiol. 133: 462-469.

Sauer, M., Paciorek, T., Benková, E., and Friml, J. (2006). Immunocytochemical techniques for whole mount *in situ* protein localization in plants. Nat. Protoc. **1:** 98-103.